Journal of Scientific Computing, Vol. 27, Nos. 1–3, June 2006 (© 2006)
DOI: 10.1007/s10915-005-9033-0

Adaptive Central-Upwind Schemes for Hamilton–Jacobi Equations with Nonconvex Hamiltonians

Alexander Kurganov[1] and Guergana Petrova[2]

Received October 22, 2004; accepted (in revised form) October 14, 2005; Published online March 22, 2006

This paper is concerned with computing viscosity solutions of Hamilton–Jacobi equations using high-order Godunov-type projection-evolution methods. These schemes employ piecewise polynomial reconstructions, and it is a well-known fact that the use of more compressive limiters or higher-order polynomial pieces at the reconstruction step typically provides sharper resolution. We have observed, however, that in the case of nonconvex Hamiltonians, such reconstructions may lead to numerical approximations that converge to generalized solutions, different from the viscosity solution. In order to avoid this, we propose a simple adaptive strategy that allows to compute the unique viscosity solution with high resolution. The strategy is not tight to a particular numerical scheme. It is based on the idea that a more dissipative second-order reconstruction should be used near points where the Hamiltonian changes convexity (in order to guarantee convergence to the viscosity solution), while a higher order (more compressive) reconstruction may be used in the rest of the computational domain in order to provide a sharper resolution of the computed solution. We illustrate our adaptive strategy using a Godunov-type central-upwind scheme, the second-order generalized minmod and the fifth-order weighted essentially non-oscillatory (WENO) reconstruction. Our numerical examples demonstrate the robustness, reliability, and non-oscillatory nature of the proposed adaptive method.

KEY WORDS: Hamilton–Jacobi equations; nonconvex Hamiltonian; central-upwind schemes; generalized minmod limiter; WENO reconstruction.

[1] Mathematics Department, Tulane University, New Orleans, LA 70118, USA. E-mail: kurganov@math.tulane.edu
[2] Department of Mathematics, Texas A&M University, College Station, TX 77843, USA. E-mail: gpetrova@math.tamu.edu

1. INTRODUCTION

We study approximate solutions of the Hamilton–Jacobi (HJ) equation:

$$\varphi_t + H(\nabla_{\mathbf{x}}\varphi) = 0, \quad \mathbf{x} \in \mathbb{R}^d, \tag{1.1}$$

computed using a class of projection-evolution methods, called Godunov-type schemes. One of the main building blocks of these schemes is a continuous piecewise polynomial interpolant based on the point values of the computed solution. At every evolution step, this interpolant is evolved to the next time level according to (1.1). We have observed that, as in the case of nonconvex hyperbolic conservation laws (see [7]), the choice of the reconstruction is crucial for capturing the *viscosity solutions* of HJ equations with nonconvex Hamiltonians (see [1, 11] and the references therein for a bird's eye view on the theory of viscosity solutions and various applications). Namely, the use of a dissipative second-order reconstruction seems to result in the convergence of the computed solution toward the viscosity solution, while more compressive and higher-order reconstructions may lead to the computation of a generalized solution, different from the viscosity solution. While this behavior is expected in the case of one-dimensional (1D) HJ equations (because of their direct relation to the corresponding scalar conservation laws and the results reported in [7]), it is completely new in the two-dimensional (2D) case, in which HJ equations and conservations laws are no longer equivalent. Notice that while dissipative reconstructions seem to ensure convergence to the physically relevant solutions, higher-order (more compressive) reconstructions typically provide sharper resolution and a better quality of the computed solutions.

In this paper, we propose a simple adaptive strategy, which follows the one in [7] and automatically switches the high- and low-order reconstructions around the points where the Hamiltonian changes convexity. This approach is not tight to a particular scheme and utilizes the advantages of both reconstructions in order to *compute the viscosity solution with high resolution*.

We illustrate this general strategy using a particular Godunov-type method–the central-upwind scheme from [2] with the dissipative second-order minmod reconstruction [8–10] and the fifth-order WENO reconstruction [3, 5]. The resulting method is referred to as *an adaptive semi-discrete central-upwind scheme*. However, we would like to point out once again that our adaptive strategy can be applied with any Godunov-type projection-evolution method and any couple of a dissipative and high-order (compressive) reconstructions.

The paper is organized as follows. In Sec. 2, we give a brief overview of the semi-discrete central-upwind schemes from [2] and describe our adaptive strategy. The numerical experiments are carried out in Sec. 3.

2. SEMI-DISCRETE CENTRAL-UPWIND SCHEMES

2.1. Brief Overview

In this section, we describe the *low-dissipative semi-discrete second-order central-upwind scheme* from [2] for the 1D HJ equation:

$$\varphi_t + H(\varphi_x) = 0, \quad x \in \mathbb{R}, \tag{2.1}$$

subject to the initial data $\varphi(x,0) = \varphi_0(x)$. For simplicity, we consider a uniform grid in space and time, setting $x_j := j\Delta x$ and $t^n := n\Delta t$. We denote the approximate value of $\varphi\left(x_j, t^n\right)$ by φ_j^n and assume that the values φ_j^n have been already computed. The solution at time $t = t^n$ is then globally approximated by a continuous non-oscillatory piecewise quadratic interpolant $\widetilde{\varphi}(x, t^n)$, which is reconstructed from φ_j^n. At every grid point, the maximal right and left speeds of propagation, a_j^+ and a_j^- ($a_j^\pm$ depend on time, $\varphi_x^\pm$ depend on both time and location, but these dependences are omitted to simplify the notation), are estimated by

$$\begin{aligned} a_j^+ &= \max_{\min\{\varphi_x^-, \varphi_x^+\} \leqslant u \leqslant \max\{\varphi_x^-, \varphi_x^+\}} \left\{ H'(u), 0 \right\}, \\ a_j^- &= \left| \min_{\min\{\varphi_x^-, \varphi_x^+\} \leqslant u \leqslant \max\{\varphi_x^-, \varphi_x^+\}} \left\{ H'(u), 0 \right\} \right|, \end{aligned} \tag{2.2}$$

where $\varphi_x^\pm$ are the one-sided derivatives at $x = x_j$, that is,

$$\varphi_x^\pm := \widetilde{\varphi}_x(x_j \pm 0, t^n).$$

The values $\varphi_x^\pm$ are given by:

$$\varphi_x^\pm = \frac{(\Delta\varphi)^n_{j\pm\frac{1}{2}}}{\Delta x} \mp \frac{\Delta x}{2} (\varphi_{xx})^n_{j+\frac{1}{2}}, \qquad (\Delta\varphi)^n_{j+\frac{1}{2}} := \varphi^n_{j+1} - \varphi^n_j, \tag{2.3}$$

where the second derivative is computed using a nonlinear limiter in order to ensure a non-oscillatory nature of the reconstruction, and thus of the resulting scheme. We use the generalized minmod limiter (see, e.g., [8–10]) to obtain

$$(\varphi_{xx})^n_{j+\frac{1}{2}} = \text{minmod}\left(\theta \frac{(\Delta\varphi)^n_{j+\frac{3}{2}} - (\Delta\varphi)^n_{j+\frac{1}{2}}}{(\Delta x)^2}, \frac{(\Delta\varphi)^n_{j+\frac{3}{2}} - (\Delta\varphi)^n_{j-\frac{1}{2}}}{2(\Delta x)^2},\right.$$
$$\left.\theta \frac{(\Delta\varphi)^n_{j+\frac{1}{2}} - (\Delta\varphi)^n_{j-\frac{1}{2}}}{(\Delta x)^2}\right). \tag{2.4}$$

In (2.4), $\theta \in [1, 2]$ and the minmod function is given by

$$\text{minmod}(x_1, x_2, \ldots) := \begin{cases} \min_j \{x_j\}, & \text{if} \quad x_j > 0 \quad \forall j, \\ \max_j \{x_j\}, & \text{if} \quad x_j < 0 \quad \forall j, \\ 0, & \text{otherwise.} \end{cases}$$

It is well-known that larger values of θ correspond to a less dissipative, more compressive reconstruction (see, e.g., [10]).

Finally, the semi-discrete central-upwind scheme from [2] can be written as the following system of ODEs:

$$\frac{d}{dt}\varphi_j(t) = -\frac{a_j^- H(\varphi_x^+) + a_j^+ H(\varphi_x^-)}{a_j^+ + a_j^-}$$
$$+ a_j^+ a_j^- \left[\frac{\varphi_x^+ - \varphi_x^-}{a_j^+ + a_j^-} - \text{minmod}\left(\frac{\varphi_x^+ - \psi_x^{\text{int}}}{a_j^+ + a_j^-}, \frac{\psi_x^{\text{int}} - \varphi_x^-}{a_j^+ + a_j^-}\right)\right], \tag{2.5}$$

where ψ_x^{int} is given by

$$\psi_x^{\text{int}} := \frac{a_j^+ \varphi_x^+ + a_j^- \varphi_x^-}{(a_j^+ + a_j^-)} - \frac{H(\varphi_x^+) - H(\varphi_x^-)}{(a_j^+ + a_j^-)}. \tag{2.6}$$

The implementation of the semi-discrete scheme (2.2)–(2.6) requires a stable ODE solver of an appropriate order. In the numerical experiments, reported in Sec. 3, we have used the third-order strong stability preserving Runge–Kutta method [4].

For further details, we refer the reader to [2], where the central-upwind scheme (2.2)–(2.6) and its multidimensional and higher-order extensions are thoroughly described.

2.2. Adaption Algorithm

First, we will try to give some insight of the observed phenomenon. The problem is best understood in the 1D case, where differentiation of the HJ equation (2.1) results in an equivalent scalar conservation law for φ_x. In the case of nonconvex H, the solution of the corresponding conservation law may develop composite waves that consist of a sequence of joint rarefactions and shocks. The use of a low dissipative reconstruction, such as the second-order one based on the generalized minmod limiter (2.4) with $\theta = 2$ or the fifth-order WENO reconstruction, enhances the influence of the shock over the rarefaction wave and thus leads to a steeper piecewise polynomial reconstruction for φ_x in the neighborhoods of shock-rarefaction junctions. The resulting overshoot/undershoot cannot be compensated by the evolution (2.5), and leads to the computation of a weak solution, different from the viscosity solution.

Next, we suggest an adaptive strategy that overcomes this difficulty:

- Use a second-order dissipative reconstruction at every point where the convexity of the Hamiltonian changes and also within K neighboring grid points (in the 2D case, this means K grid points in each direction). At these grid points, the values of the local speeds are calculated using (2.2).
- Use a high-order (compressive) reconstruction in the rest of the computational domain, where (2.2) reduces to

$$a_j^+ = \max\left\{H'(\varphi_x^-), H'(\varphi_x^+), 0\right\}, \qquad a_j^- = \left|\min\left\{H'(\varphi_x^-), H'(\varphi_x^+), 0\right\}\right|.$$

Remarks.

1. Our numerical experiments suggest that in order to ensure convergence to the viscosity solution, K should be taken proportional to $|\ln(\Delta x)|$ as the grid is refined.
2. We denote by MM1 and MM2 the minmod limiter (2.4) with $\theta = 1$ and $\theta = 2$, respectively, and by WENO5 the fifth-order WENO reconstruction. In our numerical experiments, the adaption algorithm has been realized using the MM1 as a dissipative reconstruction and the WENO5 as a higher-order one.

3. NUMERICAL EXAMPLES

In this section, we illustrate the performance of our adaptive central-upwind scheme. We show 2D examples only, since in the 1D case, the differentiation of HJ equations results in equivalent scalar conservation laws, for which the dependence of the computed solution on the reconstruction has been discovered in [7].

As our 2D numerical experiments suggest, the MM1 reconstruction consistently leads to capturing the viscosity solution, while the use of the MM2 or WENO5 reconstructions may or may not (depending on the problem solved) lead to the convergence towards the viscosity solution. The proposed adaptive scheme also consistently captures the viscosity solution since our adaptive reconstruction reduces to the MM1 reconstruction near the Hamiltonian inflection points. At the same time, it enjoys high resolution property of the WENO5 reconstruction in the rest of the computational domain. We would also like to point out that our adaptive strategy does not seem to be very sensitive to the choice of adaption constant K. In the reported numerical examples, $K=1$ in all 201×201 computations, while for the 801×801 grid $K=2$.

Example 1. We numerically solve the 2D HJ equation:

$$\varphi_t+\sin(\varphi_x)+\cos(\varphi_y)=0, \qquad (x,y)\in(-2,2)\times(-2,2), \quad t>0, \tag{3.1}$$

subject to the following radially symmetric oscillatory initial condition $\varphi(x,y,0)=\varphi_0(r)$, $r:=\sqrt{x^2+y^2}$:

$$\varphi_0(r)=\begin{cases}\frac{\pi}{4}(14r-13), & r\leqslant\frac{1}{2},\\ \frac{\pi}{4}(14r-13)+2\sin(10\pi r), & \frac{1}{2}<r\leqslant 1,\\ \frac{\pi}{4}r, & r>1,\end{cases} \tag{3.2}$$

and the homogeneous Neumann boundary conditions for φ_x and φ_y:

$$\begin{cases}\varphi_{xx}(-2,y,t)=\varphi_{xx}(2,y,t)=0, & \forall t,\ \forall y\in[-2,2],\\ \varphi_{yy}(x,-2,t)=\varphi_{yy}(x,2,t)=0, & \forall t,\ \forall x\in[-2,2].\end{cases} \tag{3.3}$$

We have computed the solution of the initial-boundary-value (IBVP) problem (3.1)–(3.3) at time $t=2$ using the MM1, MM2, WENO5, and the 2D version of our adaptive reconstruction (we refer the reader to [2, 6, 8] for a detailed description of these 2D reconstructions). For adaption, we check at every grid point whether a point where the convexity of the Hamiltonian changes is near-by (in this example, the convexity changes at the points where either $\varphi_x=k\pi$ or $\varphi_y=\ell\pi/2$, $k,\ell\in\mathbb{Z}$). If this is the case, that is, if the distance between the current grid point and one of the aforementioned inflection points is smaller than $K\max(\Delta x,\Delta y)$, the dissipative MM1 reconstruction is used at this grid point. Otherwise, the numerical Hamiltonian there is computed using the sharper WENO5 reconstruction.

Even though the exact viscosity solution of this IBVP is unavailable, it seems to be reasonable to expect that similarly to the case of hyperbolic conservation laws, studied in [7], the MM1 solution would capture the viscosity solution. In Fig. 1, we show the solutions computed on a

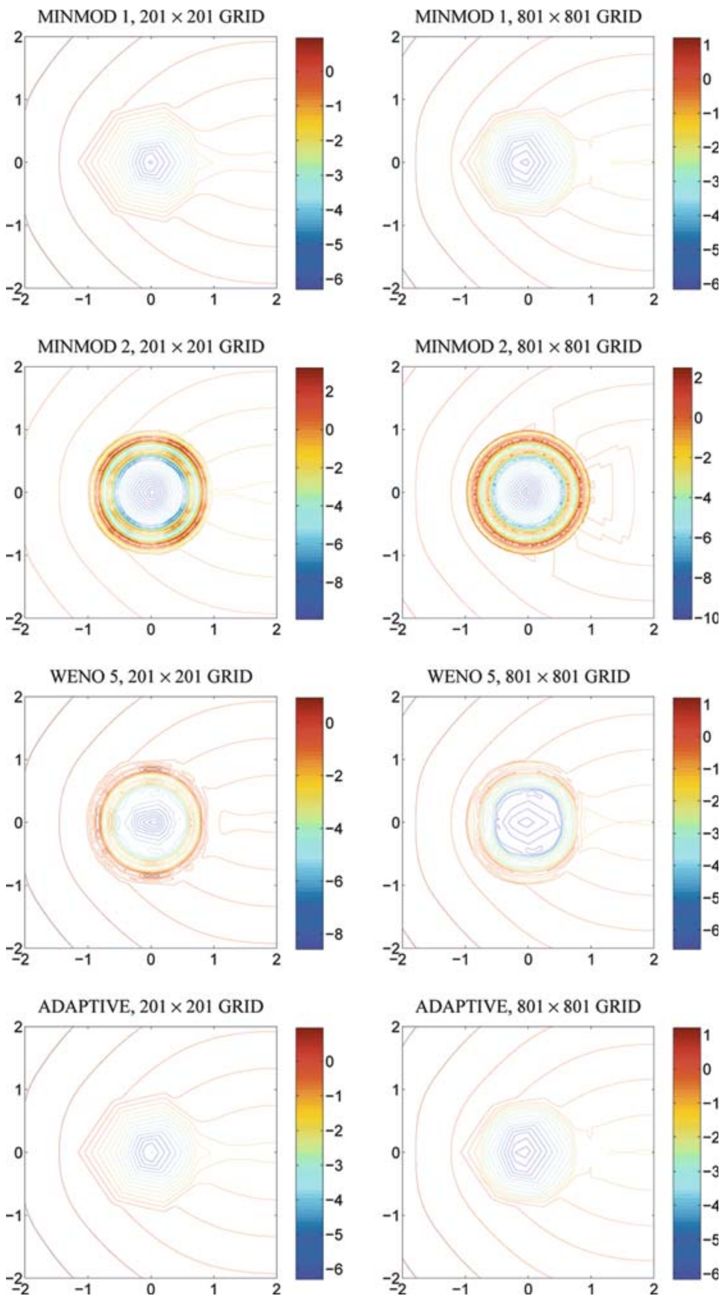

Fig. 1. Computed solutions of the IBVP (3.1)–(3.3).

relatively coarse 201×201 grid and on a much finer 801×801 grid. As one can clearly see there, the difference between the MM1, MM2 and WENO5 solutions is quite significant (both MM2 and WENO5 solutions seem to converge to generalized solutions, different from the viscosity solution). On the other hand, both the MM1 solution and the solution, computed by the adaptive central-upwind scheme, converge to what we believe to be the viscosity solution of this IBVP.

The purpose of the next example is to show that even though both the MM1 and adaptive solutions seem to converge to the viscosity solution, the adaptive solution provides higher resolution and thus justifies the proposed adaptive strategy.

Example 2. We numerically solve a different 2D HJ equation:

$$\varphi_t + \sin(\varphi_x) + \frac{1}{4}\varphi_y = 0, \qquad (x, y) \in (-2, 2) \times (-2, 2), \quad t > 0, \qquad (3.4)$$

subject to the same initial (3.2) and boundary (3.3) conditions. In this example, the initial condition undergoes a nonlinear transformation in the x-direction only, while it is being linearly advected in the y-direction. Thus, the solution preserves some of its initial oscillatory nature, which is captured much more accurately by a higher-order scheme.

As in Example 1, we compute the solution of the IBVP (3.2)–(3.4) at time $t = 2$ with 201×201 and 801×801 uniform grids using the MM1, MM2, WENO5, and the adaptive reconstruction. The contour lines of the computed solution, presented in Fig. 2, demonstrate the convergence of both the MM1 and adaptive solutions to the viscosity solution. One can only observe a superior resolution, achieved by the adaptive central-upwind scheme due to the smaller amount of numerical viscosity. We would like to mention that in this example, the WENO5 solution also seems to converge to the viscosity solution though slower than its MM1 and adaptive counterparts. Also, notice that the WENO5 solution is much more oscillatory than the MM1 and adaptive solutions.

The cross-sections at $y = 0.5$ and $x = 0$ of the MM1, WENO5 and adaptive solutions, computed with the 201×201 uniform grid are presented in Fig. 3. We also show the MM1 solution, computed on a finer 801×801 grid, which serves as a reference solution. As one could expect, the $y = 0.5$ cross-sections of the MM1 and adaptive solutions are very close (though the adaptive one is a little sharper near the extremum). However, the $x = 0$ cross-sections clearly demonstrate the advantage of the proposed adaptive strategy: in the region where the solution has an oscillatory nature, the resolution achieved by the adaptive scheme with the 201×201 grid seems to be superior to the one obtained by the second-order MM1 scheme with the 801×801 grid.

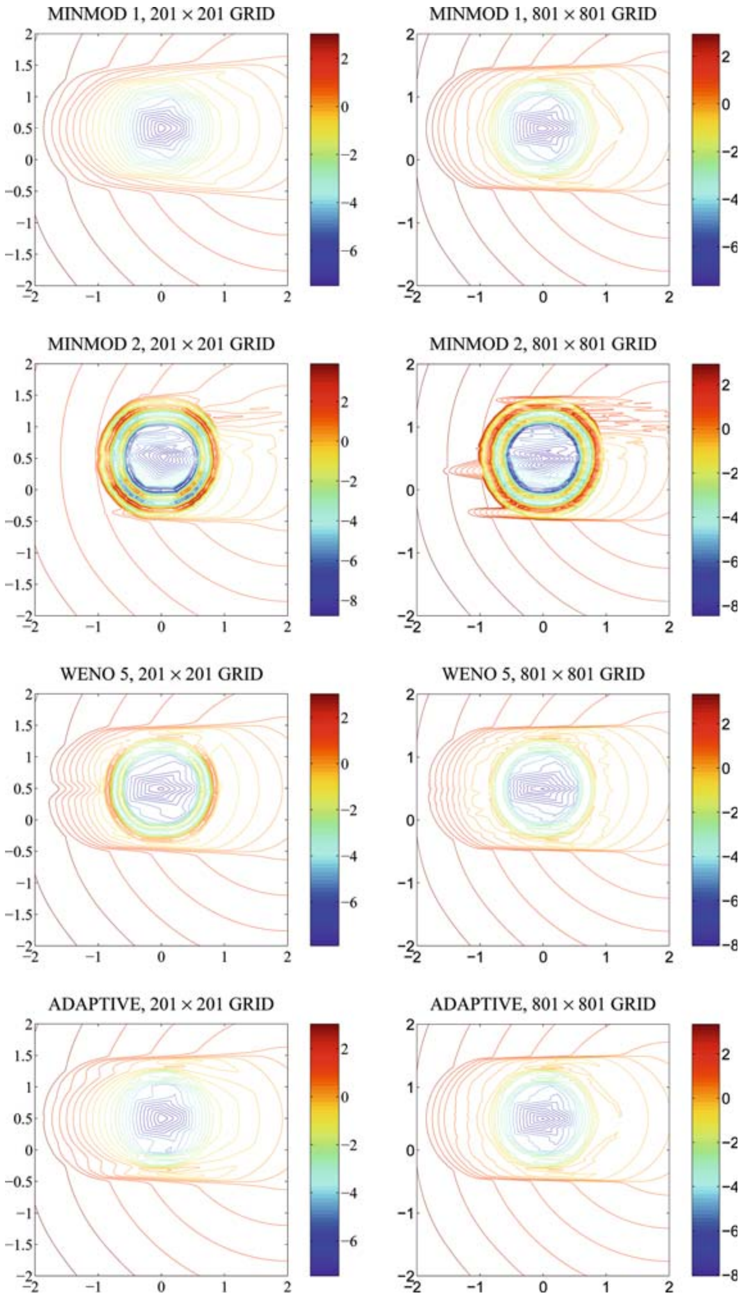

Fig. 2. Computed solutions of the IBVP (3.2)–(3.4).

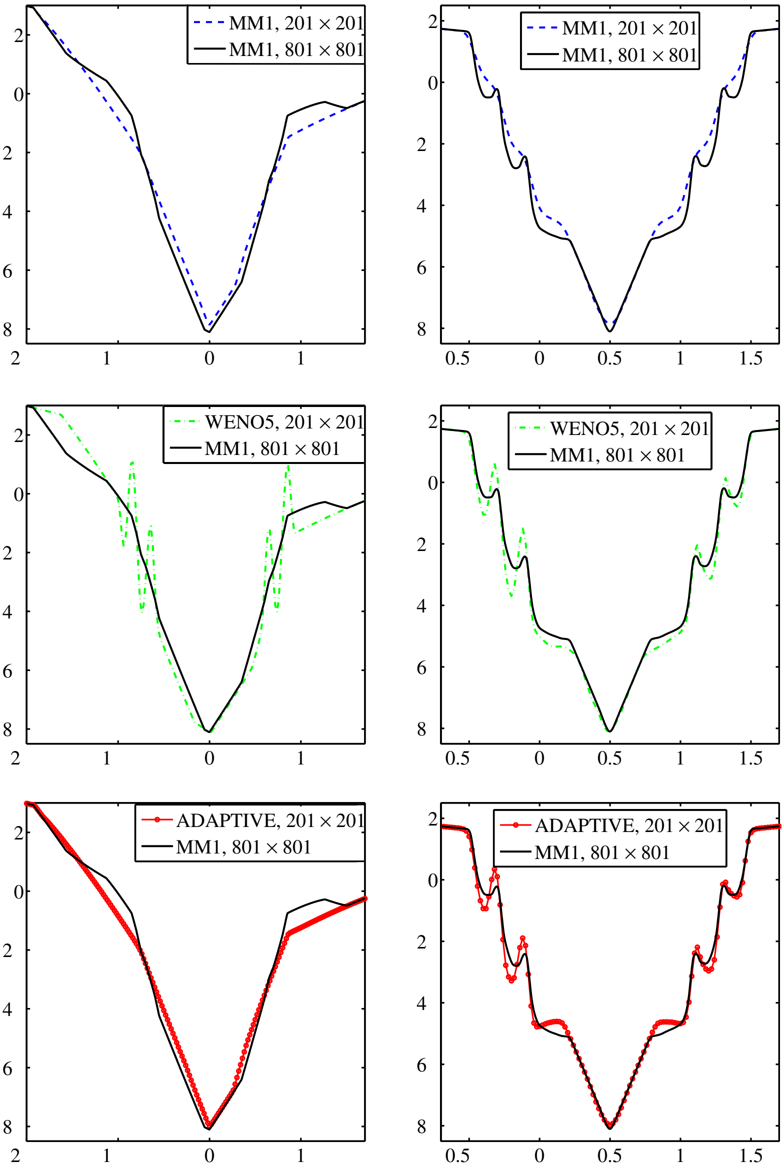

Fig. 3. Cross-sections at $y = 0.5$ (left column) and $x = 0$ (right column) of the MM1, WENO5, and adaptive solutions, computed on the 201×201 grid, and the reference MM1 solution, computed on the 801×801 grid.

ACKNOWLEDGMENT

The research of A. Kurganov was supported in part by the NSF Grant #DMS-0310585. The work of G. Petrova was supported in part by the NSF Grants #DMS-0296020 and #DMS-0505501.

REFERENCES

1. Bardi, M., Crandall, M., Evans, L., Sonar, H., and Souganidis, P. (1997). Viscosity solutions and applications. In Capuzzo Dolcetta, I. and Lions, P.-L. (eds.), Lecture Notes in Mathematics, Springer-Verlag, New York/Berlin, CIME Lecture Notes Vol. 1660.
2. Bryson, S., Kurganov, A., Levy, D., and Petrova, G. (2005). Semi-discrete central-upwind schemes with reduced dissipation for Hamilton-Jacobi equations. *IMA J. Numer. Anal.* **25**, 113–138.
3. Bryson, S., and Levy, D. (2003). High-order semi-discrete central-upwind schemes for multi-dimensional Hamilton-Jacobi equations. *J. Comput. Phys.* **189**, 63–87.
4. Gottlieb, S., Shu, C.-W., and Tadmor, E. (2001). High order time discretization methods with the strong stability property. *SIAM Rev.* **43**, 89–112.
5. Jiang, G.-S., and Peng, D. (2000). Weighted ENO schemes for Hamilton-Jacobi equations. *SIAM J. Sci. Comput.* **21**, 2126–2143.
6. Kurganov, A., Noelle, S., and Petrova, G. (2001). Semidiscrete central-upwind schemes for hyperbolic conservation laws and Hamilton-Jacobi equations. *SIAM J. Sci. Comput.* **23**, 707–740.
7. Kurganov, A., Petrova, G., and Popov, B. (submitted). Adaptive semi-discrete central-upwind schemes for nonconvex hyperbolic conservation laws. A preprint is available at `http://www.math.tulane.edu/~kurganov/pub.html`.
8. Kurganov, A., and Tadmor, E. (2000). New high-resolution semi-discrete schemes for Hamilton-Jacobi equations. *J. Comput. Phys.* **160**, 241–282.
9. van Leer, B. (1979). Towards the ultimate conservative difference scheme, V. A second order sequel to Godunov's method. *J. Comput. Phys.* **32**, 101–136.
10. Lie, K.-A., and Noelle, S. (2003). On the artificial compression method for second-order nonoscillatory central difference schemes for systems of conservation laws. *SIAM J. Sci. Comput.* **24**, 1157–1174.
11. Lions, P. (1982). Generalized solutions of Hamilton-Jacobi equations, Pitman Publishing Inc.